JACS
JOURNAL OF THE AMERICAN CHEMICAL SOCIETY

Article

pubs.acs.org/JACS

Development of a Series of Near-Infrared Dark Quenchers Based on Si-rhodamines and Their Application to Fluorescent Probes

Takuya Myochin,[†] Kenjiro Hanaoka,*[,†] Shimpei Iwaki,[†,⊥] Tasuku Ueno,[†,⊥] Toru Komatsu,[†,¶] Takuya Terai,[†] Tetsuo Nagano,[‡] and Yasuteru Urano*[,†,§,⊥]

[†]Graduate School of Pharmaceutical Sciences, [‡]Open Innovation Center for Drug Discovery, and [§]Graduate School of Medicine, The University of Tokyo, Tokyo 113-0033, Japan

[¶]PRESTO and [⊥]CREST, Japan Science and Technology Agency (JST), Saitama 332-0012, Japan

Supporting Information

ABSTRACT: Near-infrared (NIR) fluorescent probes based on the Förster resonance energy transfer (FRET) mechanism have various practical advantages, and their molecular design is generally based on the use of NIR dark quenchers, which are nonfluorescent dyes, as cleavable FRET acceptors. However, few NIR dark quenchers can quench fluorescence in the Cy7 region (over 780 nm). Here, we describe Si-rhodamine-based NIR dark quenchers (SiNQs), which show broad absorption covering this region. They are nonfluorescent independently of solvent polarity and pH, probably due to free rotation of the bond between the N atom and the xanthene moiety. SiNQs can easily be structurally modified to tune their water-solubility and absorption spectra, enabling flexible design of appropriate FRET pair for various NIR fluorescent dyes. To demonstrate the usefulness of SiNQs, we designed and synthesized a NIR fluorescent probe for matrix metalloproteinase (MMP) activity using SiNQ780. This probe **1** could detect MMP activity *in vitro*, in cultured cells and in a tumor-bearing mouse, in which the tumor was clearly visualized, by NIR fluorescence. We believe SiNQs will be useful for the development of a wide range of practical NIR fluorescent probes.

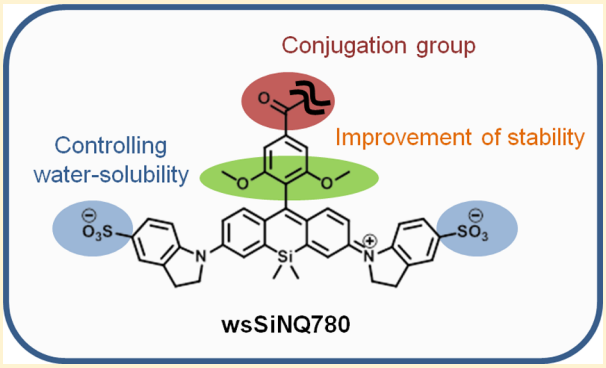

INTRODUCTION

Near-infrared (NIR) fluorescence imaging is one of the most powerful *in vivo* imaging techniques in both life sciences and medicine,[1] and activatable NIR fluorescent probes, which show a fluorescence change in response to biological events such as enzymatic activities, offer particular advantages, including high tissue transparency and low autofluorescence in the NIR region. For the molecular design of activatable fluorescent probes, several fluorescence off/on controlling mechanisms are available, such as photoinduced electron transfer (PeT), absorption spectral change and Förster resonance energy transfer (FRET).[2−4] Among them, the FRET-based design strategy can be easily applied to various fluorophores including NIR fluorescent dyes, unlike PeT or the absorption spectral change strategy, and FRET-based molecular design can achieve a low background fluorescence simply by linking a fluorophore (FRET donor) to a dark quencher, which is a nonfluorescent dye or a gold nanoparticle (FRET acceptor), via an enzyme-cleavable peptide linker,[5] while FRET is also often utilized for the ratiometric fluorescence measurement.[4d] This design strategy has also been applied to photosensitizers.[6]

NIR dark quenchers that have been reported so far include gold nanoparticle, QSY21, BHQ-3, and IRDye QC-1.[5b,7−9] However, QSY 21 and BHQ-3 do not possess a sufficiently extended absorption spectrum to quench the fluorescence of Cy7 (over 780 nm), while IRDye QC-1 shows a pH-dependent fluorescence increase below pH 5 (Figure S1). Gold nanoparticle-based quenchers are also too large for fast enzymatic reaction. So, there is a need for NIR dark quenchers that are nonfluorescent within practical ranges of solvent polarity and pH and also have sufficiently broad long-wavelength absorption to quench the fluorescence of Cy7.

Herein, we present silicon-substituted rhodamine dyes, SiNQs, as versatile dark quenchers for the development of practical NIR fluorescent probes.

RESULTS AND DISCUSSION

Design and Synthesis of SiNQs. Initially, we focused on the QSY dark quenchers (Scheme 1). The rhodamine scaffold intrinsically shows strong fluorescence, but QSYs, which contain the rhodamine scaffold bearing aromatic rings at the N atoms at the 3,6 positions of the xanthene moiety, show no fluorescence, irrespective of solvent polarity and pH.[10] The fluorescence quenching mechanism of QSYs is suggested by some papers to possibly involve a twisted intramolecular charge transfer (TICT) state,[11] owing to free rotation of the bond between the N atom and the xanthene moiety, as shown in

Received: January 8, 2015
Published: March 12, 2015

DOI: 10.1021/jacs.5b00246
J. Am. Chem. Soc. 2015, 137, 4759−4765

Scheme 1. Design Strategy for Novel NIR Dark Quenchers, SiNQs

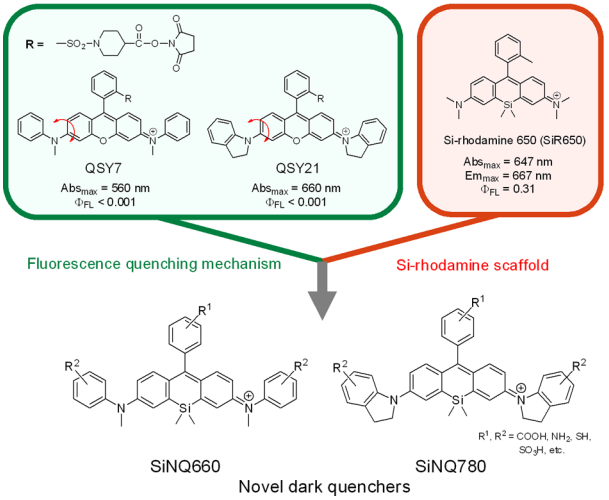

Scheme 1. We aimed to apply this fluorescence quenching strategy to far-red to NIR fluorescent dyes, Si-rhodamines (SiRs),[12] in which the O atom at the 10 position of the xanthene moiety of rhodamines is replaced with a Si atom. SiRs are rhodamine analogues with far-red to NIR absorption and fluorescence spectra and are considered amenable to a variety of structural modifications as required for biological applications. So, we set out to design and synthesize SiNQs (Si-rhodamine-based NIR dark quenchers), which contain both the Si-rhodamine scaffold and aromatic rings directly conjugated to the N atoms at the 3,6 positions of the xanthene moiety (Scheme 1).

The general synthetic route to SiRs (Scheme S1) was not suitable for the introduction of aromatic rings directly at the N atoms of the xanthene moiety. We therefore established a new general synthetic route for SiNQs as shown in Scheme 2, i.e., we first synthesized **1** according to the reported synthetic procedure of SiRs,[13] then deprotected the four allyl groups on the N atoms to obtain **2**. The amino groups of **2** were converted to iodine atoms (**3**), and anisidine or indoline was introduced at the 3,6 positions of xanthone **3** by use of the Buchwald–Hartwig reaction. Thus, compound **3** is a key intermediate for SiNQs. Finally, *o*-tolylmagnesium bromide was added to a THF solution of **4** or **6** to obtain SiNQ660 (**5**) or SiNQ780 (**7**), respectively.

Photophysical Properties. We next examined the photophysical properties of SiNQs (Table 1, Figure 1A,B). SiNQ660 (**5**) and SiNQ780 (**7**) both showed absorption in the NIR region, and their fluorescence quantum yields were almost zero (less than 0.001 in MeOH). SiNQ780 showed longer-wavelength absorption (680–850 nm) than SiNQ660, and its absorption range is suitable for quenching fluorescence in the Cy7 region via FRET. We also measured the absorption and emission spectra in various organic solvents. The fluorescence quenching ability of SiNQ660 and SiNQ780 was retained in solvents of various polarities (Figures S2, S3 and Tables S1, S2). Further, to investigate the fluorescence quenching mechanism of SiNQs, we synthesized compound **14** (Figure

Table 1. Photophysical Properties of SiNQs[a]

	Abs$_{max}$ (nm)	Em$_{max}$ (nm)	Φ_{FL}[b]
SiNQ660 (**5**)	660	n.d.	<0.001
SiNQ780 (**7**)	779	n.d.	<0.001

[a]All data were measured in MeOH. [b]For determination of the fluorescence quantum yield (Φ_{FL}), we used Cy5.5 in PBS at pH 7.4 (Φ_{FL} = 0.23) or ICG in DMSO (Φ_{FL} = 0.13) as a fluorescence standard. n.d. = not detected.

Scheme 2. Synthesis of SiNQ660 and SiNQ780[a]

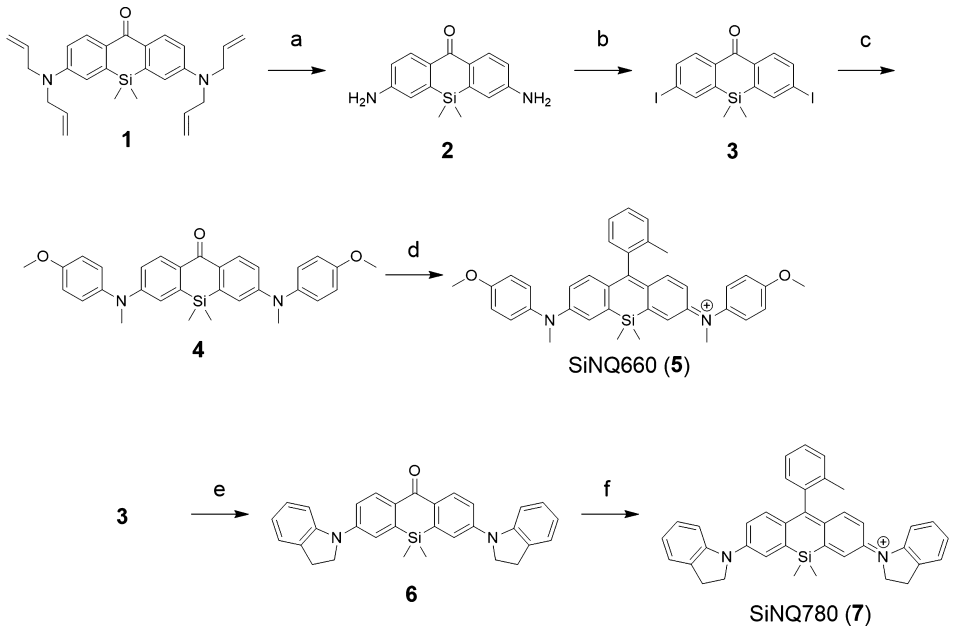

[a]Reagents and conditions: (a) $Pd(PPh_3)_4$, 1,3-dimethylbarbituric acid, CH_2Cl_2, 40 °C, 79%; (b) $NaNO_2$, KI, 2 N HCl/acetonitrile, 17%; (c) *N*-methyl-*p*-anisidine, $Pd(OAc)_2$, BINAP, Cs_2CO_3, toluene, 100 °C, 20%; (d) *o*-tolylmagnesium bromide, THF, 93%; (e) indoline, $Pd(OAc)_2$, BINAP, Cs_2CO_3, toluene, 100 °C, 54%; (f) *o*-tolylmagnesium bromide, THF, 80 °C, 30%.

DOI: 10.1021/jacs.5b00246
J. Am. Chem. Soc. 2015, 137, 4759–4765

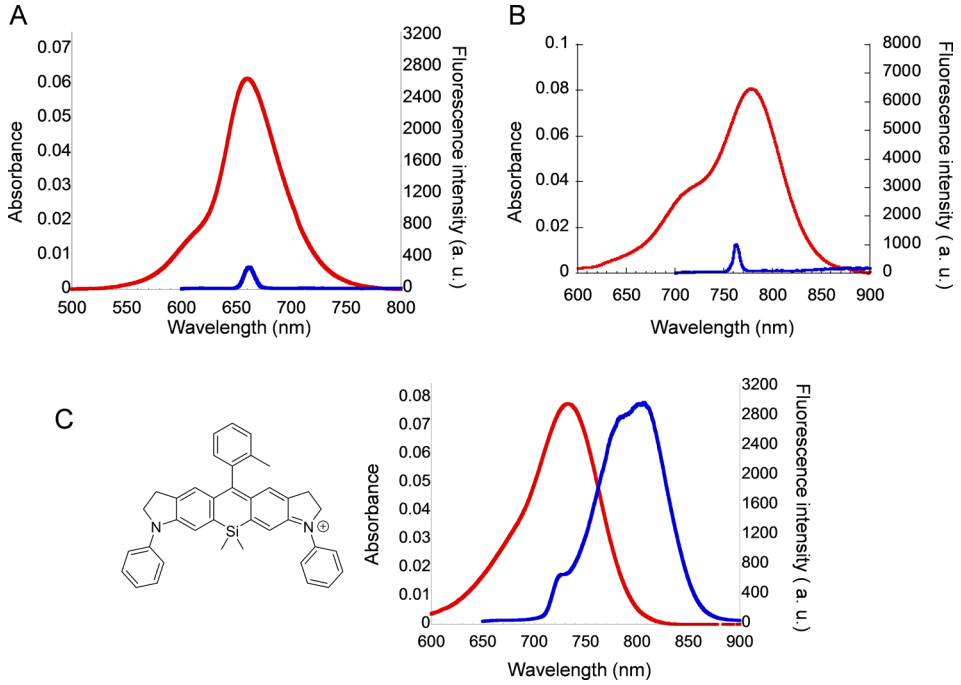

Figure 1. Absorption (red) and fluorescence (blue) spectra of SiNQ660 (**5**) (A), SiNQ780 (**7**) (B), and **14** (C) in MeOH. The excitation wavelength was 660, 760, or 720 nm, respectively. The chemical structure of **14** is shown in (C).

Scheme 3. Synthesis of wsSiNQ780 Derivatives 1, 2, and 3[a]

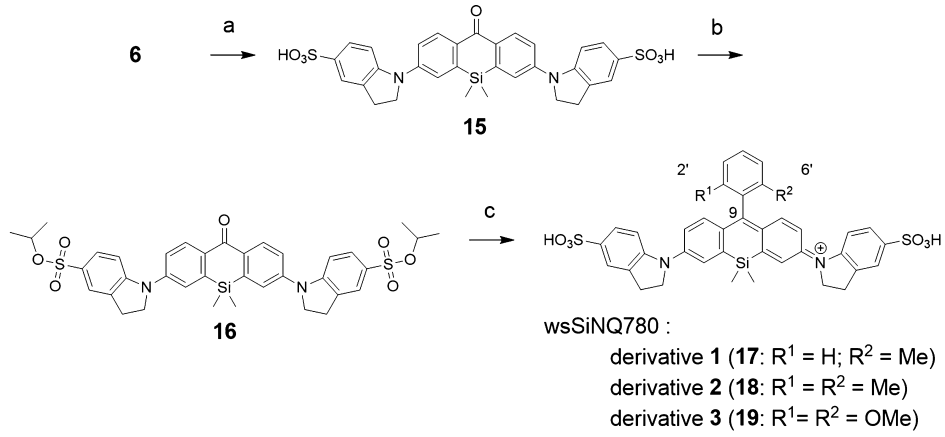

[a]Reagents and conditions: (a) $ClSO_3H$, CH_2Cl_2, 0 °C, 74%; (b) triisopropyl orthoformate, *i*-PrOH, 80 °C, 71%. (c) Derivative **1**: (i) *o*-tolylmagnesium bromide, THF, 80 °C, (ii) 2 N HCl aq., reflux, 32%. Derivatives **2** and **3**: (i) 2-bromo-*m*-xylene (dericative **2**) or 2-bromo-1,3-dimethoxybenzene (derivative **3**), *sec*-BuLi, THF, −78 °C, (ii) 2 N HCl aq., reflux, 46% (derivative **2**), 41% (derivative **3**).

1C, Scheme S2), in which rotation of the bond between the N atom and the xanthene moiety is restricted, since rotation of this bond is considered to be the main factor for the nonfluorescence of SiNQs.[11] The fluorescence quantum yield of **14** was 0.08 (Figure 1C, Table S3), so this compound was fluorescent. Therefore, we considered that the fluorescence quenching of SiNQs is mainly caused by molecular rotation around the bond between the N atom and the xanthene moiety, while the fluorescence quenching mechanism cannot still be determined to be the formation of the TICT state.

Improvement of the Water-Solubility and the Stability of the Quencher. Next, we examined the photophysical properties of SiNQ780 in sodium phosphate buffer at various pH values. However, SiNQ780 was not readily soluble in aqueous solution, so we synthesized water-soluble SiNQ780 (wsSiNQ780); i.e., to improve the water-solubility, the indoline moieties of SiNQ780 were sulfonated. The wsSiNQ780 derivative **1** (R^1 = H; R^2 = CH_3) was synthesized according to a modification of Scheme 2 (Scheme 3). The product showed good water-solubility, and its absorption spectrum was similar to that of **7** in PBS (pH 7.4), as we had expected (Figures 2A, S4). However, its absorbance unexpectedly gradually decreased in PBS (pH 7.4) during 1 h (Figure 2A). On the other hand, hardly any absorption decrease of wsSiNQ780 derivative **1** in sodium phosphate buffer at pH 3.0 was observed (Figure 2A). Therefore, we hypothesized that this absorption decrease of derivative **1** was caused by nucleophilic attack of a water molecule at the 9 position of the xanthene moiety (see Scheme 3) because the similar phenomenon was previously observed,[13b] and we set

DOI: 10.1021/jacs.5b00246
J. Am. Chem. Soc. 2015, 137, 4759−4765

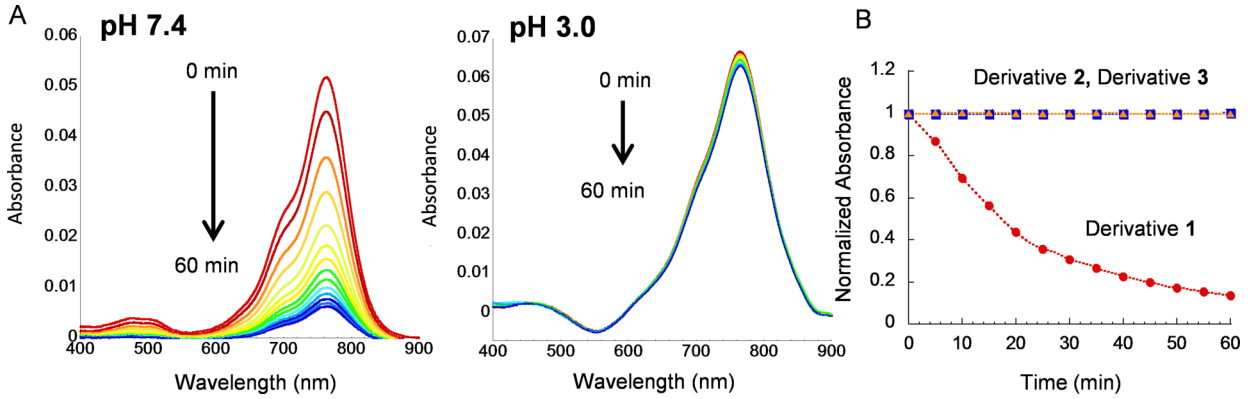

Figure 2. (A) Absorption spectral change of derivative **1** in PBS (pH 7.4) (left) and sodium phosphate buffer (pH 3.0) (right) containing 0.1% DMSO as a cosolvent. (B) Absorbance changes of derivatives **1** (circle), **2** (square), and **3** (triangle) at 780 nm in PBS (pH 7.4) containing 0.1% DMSO as a cosolvent.

Scheme 4. Synthesis of 2′,6′-dimethoxy wsSiNQ780 COOH[a]

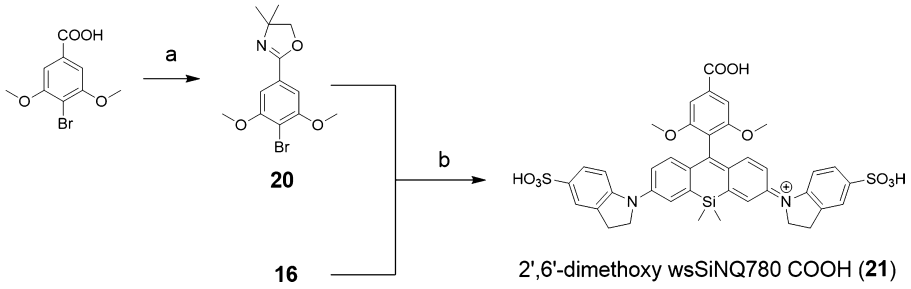

[a]Reagents and conditions: (a) PPh_3, 2-amino-2-methylpropanol, DIEA, CCl_4, pyridine, CH_3CN, 20%; (b) (i) **16**, **20**, *sec*-BuLi, THF, 60 °C, (ii) 2 N HCl aq., acetone, reflux, 2 days, 60%.

out to improve the stability of derivative **1** in aqueous solutions. For this purpose, we introduced two substituents at the 2′ and 6′ positions of the benzene moiety of wsSiNQ780; these were expected to prevent the nucleophilic attack of water through steric hindrance. We synthesized derivative **2** ($R^1 = R^2 = CH_3$) and derivative **3** ($R^1 = R^2 = OCH_3$) of wsSiNQ780 (Scheme 3) and examined their stability in aqueous solutions. These compounds showed similar absorption spectra to derivative **1** (Figure S5). The absorption of these compounds did not decrease, and these derivatives of wsSiNQ780 showed greater stability, as we had hoped (Figure 2B). We also measured the absorption and fluorescence spectra of derivative **3** in sodium phosphate buffer at various pH values. Derivative **3** showed almost no change in absorption spectra and no fluorescence, irrespective of the pH of the solution (Figure S6). Thus, we successfully developed wsSiNQ780, which has a sufficiently broad absorption spectrum in the long-wavelength region and showed high stability in aqueous solutions, with no fluorescence at any pH value in the range examined.

Application of the Quencher to NIR Fluorescent Probe. To examine the practical usefulness of wsSiNQ780 derivative **3**, we set out to develop an activatable NIR fluorescent probe for endopeptidase activity with wsSiNQ780. We selected matrix metalloproteinases (MMPs) as a target. MMPs are a family of zinc metalloproteinases that play important roles in degrading extracellular matrix and in both physiological and pathological processes of tissue remodelling.[14] Activity of MMPs is also involved in embryogenesis, wound healing, inflammation, arthritis, cardiovascular disease, and cancer.[14b,15] Among the MMPs, MMP-2 and -9 and membrane-type 1 MMP (MT1-MMP) are related to tumor invasion, metastasis, and angiogenesis, and the detection of these activities can be useful to predict the malignancy of tumors.[14a,16] To obtain the probe, we first synthesized wsSiNQ780 derivative **3** with a carboxy group at the 4′ position of the benzene moiety (Scheme 4) for conjugation to an enzymatically cleavable peptide. We also selected DY730 analogue (Figure 3A, Scheme S3), which has strong fluorescence in the Cy7 region, as a NIR fluorescent dye. A polyethylene glycol (PEG) chain (Scheme S4) was also attached to the fluorescent probe to obtain a prolonged blood-circulation time.[17] The resulting MMP probe **1**, based on the FRET mechanism, is illustrated in Figure 3A (see also Scheme S5). It was nonfluorescent ($\Phi_{FL} < 0.001$) before the enzymatic reaction, indicating that wsSiNQ780 worked well as a NIR dark quencher in the Cy7 region (Figure 3B).

Fluorescence Measurement of the Probe in Cuvette. Next, we examined whether the probe can detect MMP activity in terms of fluorescence increase in a cuvette. The probe showed a 20-fold fluorescence increase after incubation with MMP-9 or MT1-MMP catalytic domain *in vitro* (Figure 3B, S8), and enzymatic cleavage of the probe was confirmed by LC-MS analysis (Figure S9). The absorption spectrum also largely changed before and after the enzymatic reaction probably due to the stacking between the fluorescent dye and the dark quencher, wsSiNQ780. We also synthesized a control probe, MMP probe **2** (Scheme S6), which has almost the same structure as MMP probe **1**, but has D-amino acids in place of the L-amino acids in the MMP-recognition peptide motif of

DOI: 10.1021/jacs.5b00246
J. Am. Chem. Soc. 2015, 137, 4759−4765

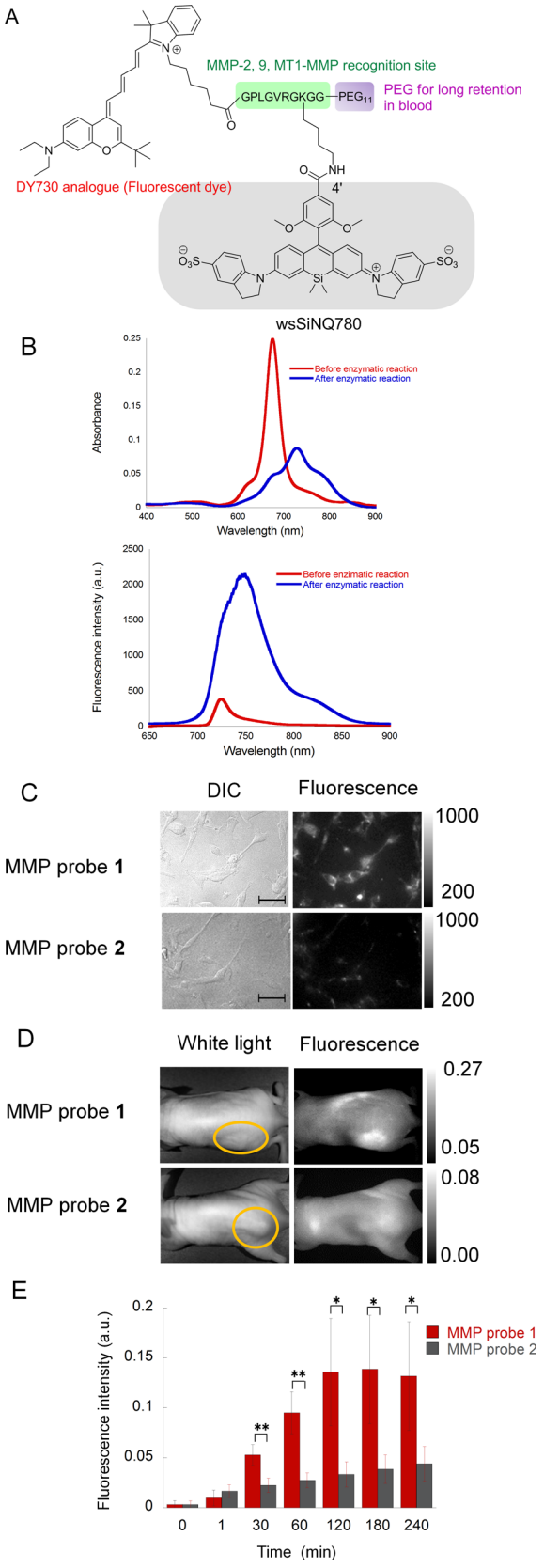

Figure 3. (A) Chemical structure of MMP probe **1**. (B) Absorption (top) and fluorescence (bottom) spectra of MMP probe **1** (final 1 μM) in TCN buffer containing 0.1% DMSO as a cosolvent. MT1-MMP catalytic domain (5 μg) was added to the solution and incubated for 2 h. Ex = 720 nm. (C) DIC and fluorescence images of HT-1080 cells exposed to MMP probe **1** or **2** (1 μM) containing 0.1% DMSO as a cosolvent in HBSS buffer. The cultured cells were incubated for 6 h after addition of the probe. Scale bar 50 μm. (D) Fluorescence images of an HT-1080 tumor-bearing nude mouse injected with MMP probe **1** or **2** (100 μM in 100 μL PBS containing 1% DMSO as a cosolvent) via the tail vein. (E) Time-dependent fluorescence change at the tumor after tail vein injection of MMP probe **1** or **2** (n = 5). Five mice were used in this experiment for each probe. $^*p < 0.05$, $^{**}p < 0.01$ Student t test.

MMP probe **1**. This probe **2** was not cleaved by MT1-MMP catalytic domain *in vitro*, as expected (Figure S7).

Live Cell Imaging with the Probe. We next applied MMP probe **1** to cultured HT-1080 cells, which express MT1-MMP on the cell surface[18] (Figure 3C). The cells were incubated with 1 μM MMP probe **1** or **2**. MMP probe **1** showed a large fluorescence increase both inside and outside the cells, i.e., the probe was cleaved outside the cells by MT1-MMP, and then the fluorophore was partially transferred into the cells because of the hydrophobicity of the DY730 analogue.[19] MMP probe **2** showed little fluorescence increase.

***In Vivo* Imaging with the Probe.** Finally, we applied MMP probe **1** to *in vivo* fluorescence imaging of MMP activity in tumor tissue (Figures 3D,E, S13). MMP probe **1** was intravenously injected into an HT-1080 tumor-bearing mouse, and the fluorescence change was monitored. The fluorescence intensity of MMP probe **1** at the tumor was clearly increased at 180 min after the probe injection. The fluorescence intensity of the tumor at 180 min was 14 times larger than that at 1 min after the probe injection. The fluorescence of the whole body was also increased, probably due to the prolonged blood retention of the cleaved (or activated) hydrophobic fluorescent probe, as already mentioned. On the other hand, the fluorescence intensity of MMP probe **2** was low after its intravenous injection, presumably because it was hardly cleaved by MMP and other endopeptidases inside the body. Thus, MMP probe **1** efficiently detected MMP activity of the tumor *in vivo*, confirming the practical usefulness of SiNQ780 as a NIR dark quencher in the Cy7 region.

Modification of the Quenchers. SiNQ780 can also easily be structurally modified to control both hydrophilicity and hydrophobicity, like wsSiNQ780 and SiNQ780 (Figure S10, Scheme S7), and the indoline moieties of SiNQ780 could also be changed to tetrahydroquinoline moieties (Figure S11, Table S4, Scheme S8). Thus, it should be straightforward to tune the chemical properties and stability of SiNQ780 as required by means of structural modification.[20] Further, for *in vivo* fluorescence imaging of endopeptidase activity, it is important to select an appropriate pair of fluorescent dye and dark quencher in order to suppress background fluorescence and to improve enzyme recognition, and the easy modifiability of SiNQ780 derivatives should allow flexible design of custom probes for particular purposes.

CONCLUSION

In summary, we have developed a series of novel dark quenchers, SiNQs, which are nonfluorescent independently of solvent polarity and pH, probably due to free rotation of the bond between the N atom and the xanthene moiety. This is important, because dark quenchers like these can work as FRET acceptors in a wide range of environments. A key advantage of SiNQ780 is that its absorption in the long-

DOI: 10.1021/jacs.5b00246
J. Am. Chem. Soc. 2015, 137, 4759−4765

wavelength is sufficient to enable it to quench Cy7 region fluorescence. We also confirmed that SiNQ780 could quench the fluorescence of ICG (Figure S12). The fact that SiNQ780 is nonfluorescent irrespective of pH represents a significant advantage over the reported NIR dark quencher IRDye QC-1, which shows strong fluorescence in low pH solutions. Furthermore, NIR fluorescent probes based on absorption change of dark quenchers have been recently reported.[7b,21] This design strategy enables us to develop fluorescent probes for various biological targets, including some that cannot be detected by using other design strategies. Therefore, SiNQs should be useful not only as versatile dark quenchers but also as a scaffold of NIR fluorescent probes for new biological targets.

EXPERIMENTAL SECTION

Materials and Methods. Reagents and solvents were of the best grade available, supplied by Tokyo Chemical Industries, Wako Pure Chemical, Aldrich Chemical Co., Biosearch Technology, Kanto Chemical Company, Watanabe Chemical Industry, and Applied Bioscience or Invitrogen, and were used without further purification. Saline was purchased from Otsuka Pharmaceutical Co. Ltd. Mice (BALB/cAJcl-nu/nu) were purchased from CLEA Japan. Reactions were monitored by means of TLC with visual observation of the dye spot or by HPLC. All compounds were purified on a silica gel column and by HPLC. All fluorescent probes were considered pure when a single HPLC peak was obtained.

Instruments. ^{1}H or ^{13}C NMR spectra were recorded on a JEOL JNM-LA300 or JMN-AL400. Mass spectra were measured with a JEOL JMS-T1000LC mass spectrometer (ESI^{+} and ESI^{-}). HPLC purifications and analyses were performed on reversed-phase columns (GL Sciences (Tokyo, Japan), Inertsil ODS-3 10 × 250 mm for purifications and Inertsil ODS-3 4.6 × 250 mm for analyses) fitted on a Jasco PU-2080 system and eluted with eluent A (H_2O containing 0.1% TFA (v/v)) and eluent B (CH_3CN with 20% H_2O containing 0.1% TFA (v/v)). Details of HPLC conditions are included in the synthesis and characterization data. Absorption spectra were obtained with a Shimadzu UV-1650 (Tokyo, Japan). Fluorescence spectroscopic studies were performed with a Hitachi F4500 (Tokyo, Japan). The slit widths were 2.5 nm for excitation and 5 nm for emission. The photomultiplier voltage was 700 V. Peptide synthesis was done on a Biotage Japan Syro-I (Tokyo, Japan). MPLC purifications were performed on a Yamazen Smart Flash EPCLC AI-5805 (Tokyo, Japan). Absolute fluorescence quantum yields were determined on a Hamamatsu Quantaurus QY C11347 (Shizuoka, Japan). LC-MS analyses were performed on an Agilent Technologies Quandrapole LC/MS 6130 1200 series.

Cell Lines and Culture Conditions. Human fibrosarcoma cell line HT-1080 was purchased from the Health Science Research Resource Bank (Osaka, Japan). HT-1080 cells were cultured in Eagle's minimal essential medium (Wako Pure Chemical), containing 1% nonessential amino acids (Invitrogen, Carlsbad, CA), 10% (v/v) fetal bovine albumin (Invitrogen Corp), and 1% penicillin (100 units/mL)-streptomycin (100 μg/mL) (Invitrogen Corp). Cells were maintained at 37 °C in a humidified incubator containing 5% CO_2.

Photophysical Properties and Fluorescence Quantum Yield. Photophysical properties of dyes were examined in PBS buffer (pH 7.4), MeOH, DMF, acetonitrile, DMSO, or chloroform containing 0.1% DMSO or 0.1% DMF as a cosolvent, using a Shimadzu UV-1650 UV−vis spectrometer and a Hitachi F4500 fluorescence spectrometer. For determination of the fluorescence quantum yield (Φ_{FL}), Cy5.5 in PBS (Φ_{FL}= 0.23)[22] or ICG in DMSO (Φ_{FL}= 0.13)[23] was used as a standard, and the results were calculated according to the following equation (subscript "st" stands for the reference and "x" for the sample).

$$\Phi_x/\Phi_{st} = [A_{st}/A_x][n_x^2/n_{st}^2][D_x/D_{st}]$$

where A is the absorbance at the excitation wavelength, n is the refractive index, and D is the area under the fluorescence spectra on an energy scale.

Stability Assessment of Compounds in Aqueous Solutions. Stability of SiNQ780 derivatives **1**, **2**, and **3** was examined in PBS (pH 7.4) containing 0.1% DMSO as a cosolvent, by using a Shimadzu UV-1650 UV−vis spectrometer.

Enzyme Assay. Five μg MMP-9 catalytic domain (human) (ENZO Life Science, USA) in 2 μL TCNB buffer (50 mM Tris, 10 mM $CaCl_2$, 150 mM NaCl, 0.05% Brij 35) (pH 7.5) or 5 μg MT1-MMP catalytic domain (human) (Calbiochem, USA) in 2 μL TCNB buffer was incubated for 15 min at 37 °C before the assay. MMP probe **1** or **2** was used at a final concentration of 1 μM in 1 mL TCN buffer (50 mM Tris, 10 mM $CaCl_2$, 150 mM NaCl, pH 7.5) containing 0.1% DMSO as a cosolvent at 37 °C. Fluorescence spectra were measured every 10 min after addition of the enzyme solution to the probe solution until the enzymatic reaction was terminated.

LC-MS Analysis. Ten μM MMP probe **1** was dissolved in 1 mL TCNB buffer containing 1% DMSO as a cosolvent, and 1 μg MMP-9 catalytic domain (ENZO Life Science) was added to the solution. The mixture was then incubated at 37 °C for 18 h. After that, the solution was lyophilized, and 30 μL H_2O was added to the residue. The solution was analyzed by LC-MS on a reversed-phase column (GL Sciences (Tokyo, Japan), Inertsil ODS-3 2.1 × 250 mm). LC-MS analysis; eluent, a 20 min linear gradient from 20% to 100% solvent B; flow rate, 0.5 mL/min; detection wavelength, 680 nm; detection MS, m/z = 904, 958, 1402.

Live Cell Imaging. HT-1080 cells seeded in an 8-well chamber (Thermo Scientific, USA) were washed with PBS and then 200 μL HBSS was added. The cells were incubated at 37 °C for 15 min. After that, MMP probe **1** or **2** (final 1 μM) was added, and incubation was continued at 37 °C for 6 h. Fluorescence images were captured without washing out excess probe, using an Olympus IX 71 with a cooled CCD camera (Coolsnap HQ, Olympus) and a xenon lamp (AH2RX-T, Olympus) with a Cy7 excitation filter and a Cy7 emission filter.

***In Vivo* Fluorescence Imaging.** All procedures were approved by the Animal Care and Use Committee of The University of Tokyo. After tail vein injection of 100 μM MMP probe **1** or **2** in 100 μL PBS containing 1% DMSO as a cosolvent, bright-field and fluorescence images were captured at different time points with a Maestro In-vivo Imaging System (CRi Inc., Woburn, MA), with an excitation filter of 671−705 nm, an emission filter of 760−770 nm, and bright-field setting. All image analyses were performed using ImageJ (NIH, Bethesda, MD, USA).

Mouse Model. All procedures were approved by the Animal Care and Use Committee of The University of Tokyo. Fluorescence imaging with MMP probe **1** or **2** was performed in BALB/cAJcl-nu/nu mice (6−7 weeks, ♀) bearing a HT-1080 xenograft tumor prepared by injection of two million HT-1080 cells into the left hind leg at 7−14 days before the fluorescence imaging experiment.

ASSOCIATED CONTENT

Supporting Information

Synthesis, experimental details and characterization of compounds, *in vitro* assays, LC-MS analysis. These materials are available free of charge via the Internet at http://pubs.acs.org.

AUTHOR INFORMATION

Corresponding Authors

*uranokun@m.u-tokyo.ac.jp
*khanaoka@mol.f.u-tokyo.ac.jp

Notes

The authors declare no competing financial interest.

DOI: 10.1021/jacs.5b00246
J. Am. Chem. Soc. 2015, 137, 4759−4765

■ ACKNOWLEDGMENTS

This work was supported in parts by MEXT (Specially Promoted Research grant nos. 22000006 to T.N., grant nos. 24689003, 24659042, and 26104509 to K.H.), SENTAN, JST to K.H. K.H. was also supported by The Asahi Glass Foundation, The Uehara Memorial Foundation, Tokyo Biochemical Research Foundation, Mochida Memorial Foundation for Medical and Pharmaceutical Research, The Naito Foundation and Takeda Science Foundation. T.M. was supported by a Grant-in-Aid for JSPS Fellows.

■ REFERENCES

(1) (a) Weissleder, R.; Pittet, M. J. *Nature* **2008**, *452*, 580−589. (b) Vahrmeijer, A. L.; Hutteman, M.; van der Vorst, J. R.; van de Velde, C. J.; Frangioni, J. V. *Nat. Rev. Clin. Oncol.* **2013**, *10*, 507−518. (c) Verbeek, F. P.; van der Vorst, J. R.; Schaafsma, B. E.; Hutteman, M.; Bonsing, B. A.; van Leeuwen, F. W.; Frangioni, J. V.; van de Velde, C. J.; Swijnenburg, R. J.; Vahrmeijer, A. L. *J. Hepatobiliary Pancreatic Sci.* **2012**, *19*, 626−637. (d) Yuan, L.; Lin, W.; Zheng, K.; He, L.; Huang, W. *Chem. Soc. Rev.* **2013**, *42*, 622−661.

(2) (a) Sasaki, E.; Kojima, H.; Nishimatsu, H.; Urano, Y.; Kikuchi, K.; Hirata, Y.; Nagano, T. *J. Am. Chem. Soc.* **2005**, *127*, 3684−3685. (b) Yu, F.; Li, P.; Li, G.; Zhao, G.; Chu, T.; Han, K. *J. Am. Chem. Soc.* **2011**, *133*, 11030−11033. (c) Yu, F.; Li, P.; Wang, B.; Han, K. L. *J. Am. Chem. Soc.* **2013**, *135*, 7674−7680.

(3) (a) Koide, Y.; Urano, Y.; Hanaoka, K.; Terai, T.; Nagano, T. *J. Am. Chem. Soc.* **2011**, *133*, 5680−5682. (b) Yuan, L.; Lin, W.; Yang, Y.; Chen, H. *J. Am. Chem. Soc.* **2012**, *134*, 1200−1211. (c) Yuan, L.; Lin, W.; Zhao, S.; Gao, W.; Chen, B.; He, L.; Zhu, S. *J. Am. Chem. Soc.* **2012**, *134*, 13510−13523.

(4) (a) Blum, G.; Mullins, S. R.; Keren, K.; Fonovic, M.; Jedeszko, C.; Rice, M. J.; Sloane, B. F.; Bogyo, M. *Nat. Chem. Biol.* **2005**, *1*, 203−209. (b) Li, J.; Chen, K.; Liu, H.; Cheng, K.; Yang, M.; Zhang, J.; Cheng, J. D.; Zhang, Y.; Cheng, Z. *Bioconjugate Chem.* **2012**, *23*, 1704−1711. (c) Ogawa, M.; Kosaka, N.; Choyke, P. L.; Kobayashi, H. *Bioconjugate Chem.* **2009**, *20*, 147−154. (d) VanEngelenburg, S. B.; Palmer, A. E. *Curr. Opin. Chem. Biol.* **2008**, *12*, 60−65.

(5) (a) Razkin, J.; Josserand, V.; Boturyn, D.; Jin, Z. H.; Dumy, P.; Favrot, M.; Coll, J. L.; Texier, I. *ChemMedChem* **2006**, *1*, 1069−1072. (b) Chen, W.-H.; Xu, X.-D.; Jia, H.-Z.; Lei, Q.; Luo, G.-F.; Cheng, S.-X.; Zhuo, R.-X.; Zhang, X.-Z. *Biomaterials* **2013**, *34*, 8798−8807.

(6) Lovell, J. F.; Chen, J.; Jarvi, M. T.; Cao, W. G.; Allen, A. D.; Liu, Y.; Tidwell, T. T.; Wilson, B. C.; Zheng, G. *J. Phys. Chem. B* **2009**, *113*, 3203−3211.

(7) (a) Stabley, D. R.; Jurchenko, C.; Marshall, S. S.; Salaita, K. S. *Nat. Methods* **2012**, *9*, 64−67. (b) Takahashi, S.; Piao, W.; Matsumura, Y.; Komatsu, T.; Ueno, T.; Terai, T.; Kamachi, T.; Kohno, M.; Nagano, T.; Hanaoka, K. *J. Am. Chem. Soc.* **2012**, *134*, 19588−19591.

(8) Johansson, M. K.; Cook, R. M. *Chem.—Eur. J.* **2003**, *9*, 3466−3471.

(9) Peng, X. X.; Chen, H. X.; Draney, D. R.; Volcheck, W.; Schutz-Geschwender, A.; Olive, D. M. *Anal. Biochem.* **2009**, *388*, 220−228.

(10) Jeon, J.; Lee, K. H.; Rao, J. *Chem. Commun.* **2012**, *48*, 10034−10036.

(11) (a) Vogel, M.; Rettig, W.; Sens, R.; Drexhage, K. H. *Chem. Phys. Lett.* **1988**, *147*, 452−460. (b) Jones, G., II; Jackson, W. R.; Choi, C. *J. Phys. Chem.* **1985**, *89*, 294−300.

(12) Koide, Y.; Urano, Y.; Hanaoka, K.; Terai, T.; Nagano, T. *ACS Chem. Biol.* **2011**, *6*, 600−608.

(13) (a) Egawa, T.; Koide, Y.; Hanaoka, K.; Komatsu, T.; Terai, T.; Nagano, T. *Chem. Commun.* **2011**, *47*, 4162−4164. (b) Kushida, Y.; Hanaoka, K.; Komatsu, T.; Terai, T.; Ueno, T.; Yoshida, K.; Uchiyama, M.; Nagano, T. *Bioorg. Med. Chem. Lett.* **2012**, *22*, 3908−3911.

(14) (a) Gialeli, C.; Theocharis, A. D.; Karamanos, N. K. *FEBS J.* **2011**, *278*, 16−27. (b) Chakraborti, S.; Mandal, M.; Das, S.; Mandal, A.; Chakraborti, T. *Mol. Cell. Biochem.* **2003**, *253*, 269−285.

(15) (a) Shiomi, T.; Lemaître, V.; D'Armiento, J.; Okada, Y. *Pathol. Int.* **2010**, *60*, 477−496. (b) Egeblad, M.; Werb, Z. *Nat. Rev. Cancer* **2002**, *2*, 161−174.

(16) (a) Itoh, Y.; Seiki, M. *J. Cell. Physiol.* **2006**, *206*, 1−8. (b) Visse, R.; Nagase, H. *Circ. Res.* **2003**, *92*, 827−839.

(17) Zhu, L.; Xie, J.; Swierczewska, M.; Zhang, F.; Quan, Q.; Ma, Y.; Fang, X.; Kim, K.; Lee, S.; Chen, X. *Theranostics* **2011**, *1*, 18.

(18) Zhao, T.; Harada, H.; Teramura, Y.; Tanaka, S.; Itasaka, S.; Morinibu, A.; Shinomiya, K.; Zhu, Y.; Hanaoka, H.; Iwata, H.; Saji, H.; Hiraoka, M. *J. Controlled Release* **2010**, *144*, 109−114.

(19) Myochin, T.; Hanaoka, K.; Komatsu, T.; Terai, T.; Nagano, T. *J. Am. Chem. Soc.* **2012**, *134*, 13730−13737.

(20) Kong, Y.; Yao, H.; Ren, H.; Subbian, S.; Cirillo, S. L.; Sacchettini, J. C.; Rao, J.; Cirillo, J. D. *Proc. Natl. Acad. Sci. U. S. A.* **2010**, *107*, 12239−12244.

(21) Kiyose, K.; Hanaoka, K.; Oushiki, D.; Nakamura, T.; Kajimura, M.; Suematsu, M.; Nishimatsu, H.; Yamane, T.; Terai, T.; Hirata, Y.; Nagano, T. *J. Am. Chem. Soc.* **2010**, *132*, 15846−15848.

(22) Mujumdar, S. R.; Mujumdar, R. B.; Grant, C. M.; Waggoner, A. S. *Bioconjugate Chem.* **1996**, *7*, 356−362.

(23) Benson, R. C.; Kues, H. A. *J. Chem. Eng. Data* **1977**, *22*, 379−383.

DOI: 10.1021/jacs.5b00246
J. Am. Chem. Soc. 2015, 137, 4759−4765